

## COMPARATIVE ANALYSIS AND MODELLING OF NEWLY DEVELOPED AND UNCONVENTIONAL PROCESSES OF PLASTIC FORMING OF TOOTHED GEAR ELEMENTS

The article reports the results of a comparative analysis made for three novel unconventional gear wheel forging processes based on the authors' patented [5,6,21] plastic forming methods developed chiefly for the purposes of extruding hollow products as well as valves and pins. These processes are distinguished by the fact that part of the tooling elements which are normally fixed during conventional forging are purposefully set in motion. This is intended to change the conditions of friction at the metal-tool contact surface and to induce additional thermal effects due to the transformation of the plastic deformation energy into thermal energy and, as a consequence, to improve the plastic flow of metal and to reduce the force parameters of the process.

*Keywords:* forging, gears, FEM analysis, hot extrusions

### 1. Introduction

The gear wheel is one of the constructionally simpler components of drive systems, as it consists of three basic parts, such as a toothed rim, a hub and a link that connects the above-mentioned parts together. This is an indispensable element of any toothed gear, but it is also included in mechanisms, such as the coupling of the gear pump [1,2].

Gear wheels are divided into cylindrical gears and bevel gears, each of them being also classified by the style of teeth used in its construction. Gear wheels available in the metal products market include cylindrical gears with a straight, skew, chevron or helical tool line; and straight, skew and spiral bevel gears. Their application is dependent on the designation and future use of a given gear wheel. From among the various methods of toothing plastic working, forging and rolling are of the greatest importance [3,4].

Forging of gear wheels is a relatively difficult technique. To start up the production of gears with forged toothing, it is necessary above all to provide the forging shop with comprehensive solutions related to forging itself, reheating, making dies and finishing treatment.

Bevel gears with a helical tooth line are most commonly used for the manufacture of hypoid gears and are produced using appropriate machine tools. The cost of purchasing such machine tools complete with appropriate software and tooling reaches above one million dollars a piece. As can be seen, using this type of machine tools for piece production, as well as small- or medium-lot production is not economically justified – principally, they should be used for large-lot and mass production.

The present study proposes methods of forging and extruding straight, skew and spiral bevel gears using the authors' patented plastic forming schemes [5,6]. The movable (displacing or rotating) tools are designed to reduce the forging force and to fill the impression faster and more accurately at the lowest possible process temperature. In addition, the proposed forging processes have been compared with other known gear forming schemes, such as orbital forging and split die forging.

A wide range of different forming schemes can be found in both the domestic and foreign literature [7-12], which can also be used for manufacturing gear wheel and tool forgings. In many variants, they are very ingenious and productive. Developing new or improving existing materials processing technologies should consequently result in a considerable improvement in process economics, and in particular:

- an increase in material yield (the smallest possible waste),
- a reduction in energy-force parameters,
- minimizing the number of operations, including a shortening of their duration to enhance the efficiency of the entire process, and
- a lowering of the initial stock temperature [13-17].

As part of the analysis of the addressed issues of plastic forming bevel gears with different toothing forms, numerical modelling was carried out in Forge<sup>®</sup>3D, a software program relying on the finite element method [18-20].

The subject of the analysis was the effect of applying the authors' novel forging schemes on the distribution of temperature in the forging, the plastic flow of material in the die impression and the forging and extrusion force.

\* CZESTOCHOWA UNIVERSITY OF TECHNOLOGY, INSTITUTE OF METAL FORMING AND SAFETY ENGINEERING, 42- 200 CZESTOCHOWA, 19 ARMII KRAJOWEJ STR., POLAND

# Corresponding author: jm@wip.pcz.pl

## 2. The essence of the proposed author's solutions

The rotary die gear forging method relies on the methods of upsetting the stock in one flat semi-implosion that does not sink into the impression. The fundamental difference in the proposed method is that the die with the impression is set in either rotational or oscillatory motion during the operation of the punch. Figure 1. shows the schematic diagram of the gear forging method using a rotary die [6].

Perform 1 in the form of a bar (in this example, of a diameter of  $\phi 30$  mm) is placed in die 2 having a gear wheel die cavity in it. Die 2 and sleeve 3 are mounted in container 6 and have impressions on their perimeters, in which balls 7 are seated. Balls 7 perform the role of a bearing and enable the rotation of die 2 around its own axis (Fig. 1c). Figure 1c shows a conceptual 3D model of the tool for carrying out the process of forging a gear wheel with helical tothing.

By acting downwards, punch 5 upsets stock material 1, while the rotating die induces its rotation particularly in the die

impression region. After punch 5 has reached the assumed distance from the die, stock material 1 will fill the entire die cavity.

The inverted conical die gear wheel forging method is the authors' method [21]. It involves slidable through-bore sleeve 2 positioned in cylindrical container 1, with slidable through die 3 placed on top of it. Die 3 has channel 4 with an inner diameter similar to the diameter of the stock. Die 3 has also chamber 5 with walls corresponding to the form of the external surface of the ribs. The outer walls of chamber 5 and die 3 are convergent towards upper punch 9. Items 2 and 3 are initially immobilized by lock 6, and stock 7 is put in their centric openings of identical diameters. Stock 7 is restricted at the bottom by immobilized punch 8, while channel 4 of die 3 has stock 7 and upper punch 9 with flange 10 all fitted in it [21].

Chamber 5 of slidable die 3, in which stock 7 is placed, has a wall shape corresponding to the form of the outer surface of the ribbed product. The inner walls must have cavity convergent towards upper punch 9. Die 3 is terminated with channel 4 in which stock 7 and punch 9 are fit mounted. Punch 9 is provided

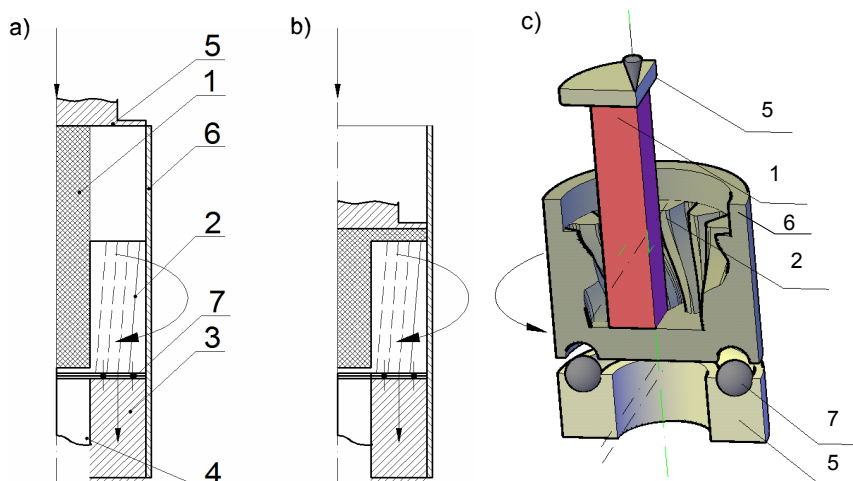


Fig. 1. Schematic diagram of the gear forging method using a rotary die; a) initial state, b) finished product, c) tool model for numerical computation

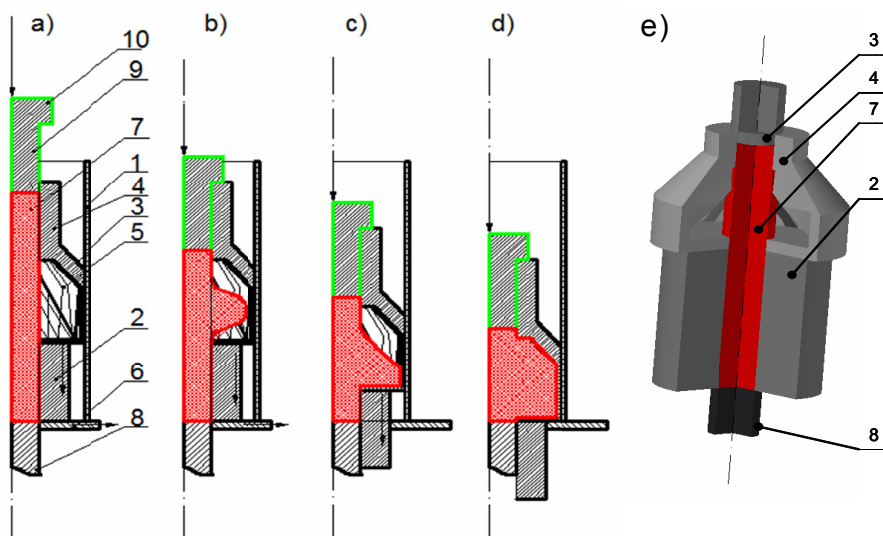


Fig. 2. Schematic diagram of the process; a) initial state, b) upsetting in the chamber, c) radial extrusion, d) finished product, e) model CAD of the tool for simulation of the inverted conical die gear forging process

with flange 10 at its end, whose job is to exert pressure onto die 3 and through-bore sleeve 2 after having preliminarily upset the stock. The punch should move them in a sliding manner within container 1, after prior releasing lock 6.

Placed in so constructed die 3 and through-bore sleeve 2 of cylindrical container 1, stock 7 is pressed by upper punch 9. The pressure causes localized upsetting in the cylindrical part of die 3. The lower zone of the impressions of chamber 5 is then completely filled. Next, lock 6 is removed, and continuing pressure on stock 7 with flange 10 of punch 9, die 3 and through-bore sleeve 2 are simultaneously moved. Radial and indirect extrusion of a ribs takes place in the impressions of chamber 5 of die 3 until the chamber is completely filled, with punch 8 being immobilized.

The inverted conical die gear wheel forging method distinguishes itself in that the extrusion process is essentially composed of two steps [5]. The steps are performed in a single punch operation. At the first step (Fig. 3b), there occurs the process of localized pre-upsetting of the bar section, whose length should not be greater than three times the diameter. At the second step (Fig. 3c,d), the die connected with the retaining ring moves downwards, and its chamber is filled with the heated-up bar being deformed on an ongoing manner.

The presented novel gear wheel extrusion method is a process whereby stock 1 in the form of a bar is placed inside die 2 and sleeve 3 that are initially immobile and connected with one another. From the bottom, stock 1 is restricted by fixed punch 4. From the top, the stock is deformed by punch 5. The whole instrumentation is housed in container 6. Initially acting on stock 1, punch 5 upsets the bar length situated outside the die. The upper die part is gradually filled with the metal being upset. After attaining the relevant distance of punch 5 from die 2, which corresponds to the thickness of the radiator base, the process proceeds to the second step. At step 2 (Fig. 3 b, c), by means of the press ejector, die 2 and sleeve 3 move downwards at a speed equal to that of punch 5, while punch 4 still remains motionless. It is important in the extrusion process that the distance between

punch 5 and die 2 do not change. Under the pressure of punch 5, the deformed metal flows radially and fills the chamber of die 2. The process will be completed when sleeves 3 has become flush with punch 4 (Fig. 3d).

### 3. Assumptions for the numerical studies

Numerical modelling of the process of gear wheel manufacture by the method of forging in the rotary die, in the inverted conical dies and in the slidable die was carried out using Forge®3D, a software program based on the FINITE ELEMENT METHOD (FEM).

The model material for forging the gear wheels shown in Figs. 1-3 was the AlMgSi (PA38) aluminium alloy. The aluminium alloy commercially marked as AW-6060 is characterized by average tensile strength and average fatigue strength. It is weldable and lends itself to decorative anodizing. It is widely used for production of aluminium bars and sections. Its high drawability, extrudability and forgeability enable products in complex shapes to be manufactured. This alloy finds application in the manufacture of architectural elements, such as window and door sections, wall elements; it is used for production of interior decoration elements, frames, lightings, ladders, railings, fences, radiators, trailer and semi-trailer parts, office equipment, car furniture, etc. Aluminium AW-6060 is offered for sale, e.g., in the form of common 20 and 30-mm diameter bars, which also contributed to the choice of this particular material. The initial temperature of the perform was  $T_0 = 500^\circ\text{C}$ , and that of the tools,  $T_n = 250^\circ\text{C}$ . The rheological properties of the model AlMgSi material were taken from the database of the Forge®3D 2011 numerical program. For the computation of the yield stress magnitude, the values of the coefficients were taken from the Forge®3 program material database. For the AlMgSi alloy, respective coefficients assume the following values:  $A = 317.6$ ,  $m_1 = -0.00429$ ,  $m_2 = 0.055$ ,  $m_3 = 0.089$ ,  $m_4 = 0$ ,  $m_5 = 0$ ,  $m_7 = 0$ ,  $m_8 = 0$ ,  $m_9 = 0$ .

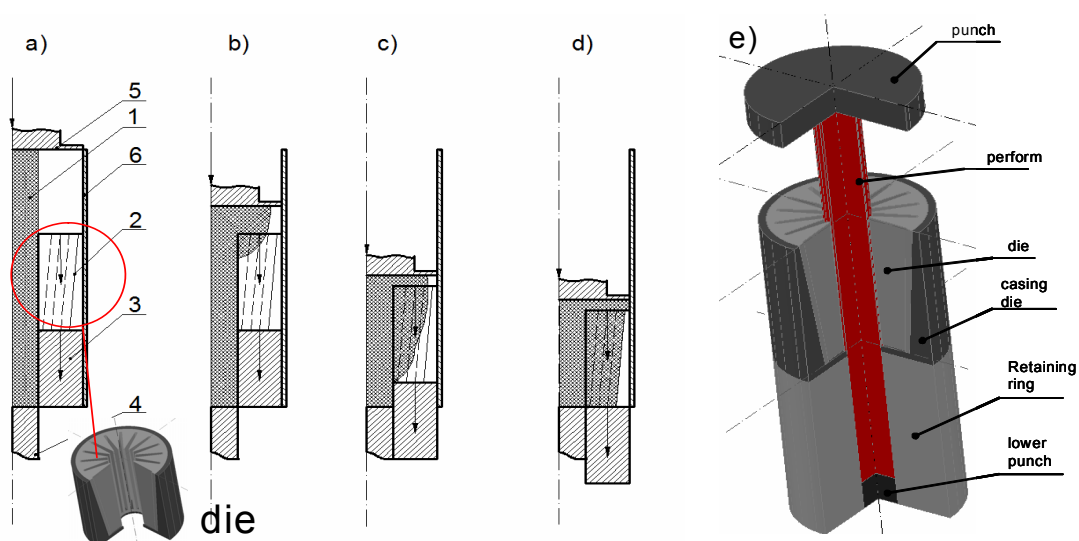


Fig. 3. Schematic diagram and the model of the tool for simulation of the conical slidable die forging process; a) initial state, b) bar flat die upset forging, c) radial extrusion, d) finished product, e) model of the tool for numerical process analysis

Forge<sup>®</sup>3D 2011 numerical program [4]. For solving the problems of three-dimensional plastic metal flow during extrusion, a mathematical model [7] was selected, in which the mechanical state of the material being deformed was described using the Norton-Hoff law [13,14], which can be expressed with the equation below:

$$S_{ij} = 2K(T, \dot{\varepsilon}, \varepsilon)(\sqrt{3} \dot{\varepsilon})^{m-1} \dot{\varepsilon}_{ij} \quad (1)$$

where:

$S_{ij}$  – stress tensor deviator, [10]

$\dot{\varepsilon}$  – strain rate intensity,

$\varepsilon_{ij}$  – strain rate tensor,

$\varepsilon$  – strain intensity,

$T$  – temperature,

$K$  – consistence dependent on the yield stress,  $\sigma_p$ ,

$m$  – coefficient characterizing hot metal deformation ( $0 < m < 1$ ).

The yield stress value is determined from the following formula [15]:

$$\sigma_p = A e^{mT} \varepsilon^{m2} \dot{\varepsilon}^{m3} \frac{m4}{\varepsilon} (1 + \varepsilon)^{m5T} \varepsilon^{m7\varepsilon} \dot{\varepsilon}^{m8T} T^{m9} \quad (2)$$

Due to the high strain intensity and the large strain value that occur during the formation of the radiator, Treska's friction

model was used for numerical computations. The value of friction factor  $m_{bare}$  0.55. The process was run at a punch and die feed rate of  $v = 20$  mm/s, while the die rotational speed amounted to  $\omega = 10$  rpm, respectively. Punch movement and rotational movement die is constant. These parameters have been selected only for numerical modeling. The perform for modelling of gear wheel forging was bar of a diameter of  $\phi = 30$  mm. Tools in numerical modelling were implemented as rigid.

#### 4. Numerical analysis and computation results

##### *The rotary die forging process*

Figure 4 a,b illustrates the results of test simulations of two gear wheel types, namely with a) straight and b) spiral toothing, on the assumption that the punch feed rate is  $v = 20$  mm/s, and die rotational speed is  $\omega = 20$  rpm.

Figure 5 shows the degree of fill of the lower die impression zone, in the sample variant with an immobile die and a rotary die for the case of forging a gear with spiral toothing.

Since this is not the temperature distribution and the filling degree of the pattern, the scale is not shown in Fig. 5.

The numerical computations represented in Fig. 5 indicate that setting the die in rotary motion causes a faster and earlier

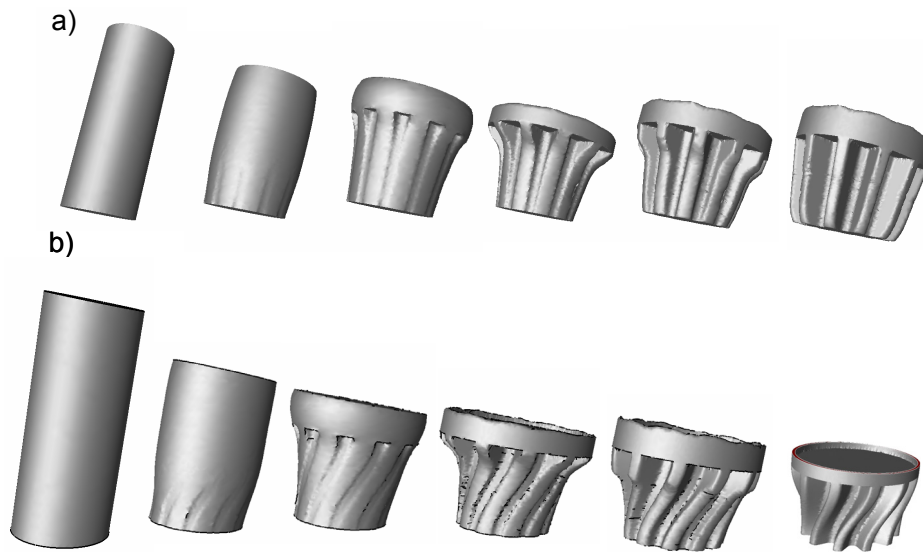


Fig. 4. Modelling numerical of the process of forging gears wheels with a) straight and b) skew toothing

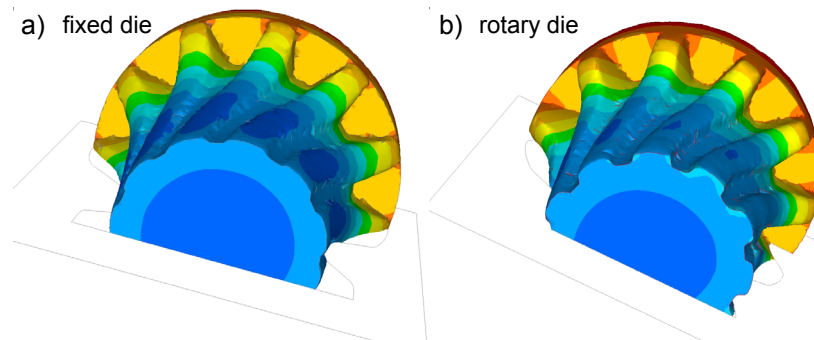


Fig. 5. Die impression fill with the analogous punch position for spiral toothing: a) immobile die, b) rotary die

impression fill. Thus, the formation of the gear toothing proceeds much quicker. The material flow is faster when the die performs rotational motion, then in the case of using an immobile tool. This is undoubtedly caused by factors, such as the occurrence of additional stresses and redundant strains in the planes perpendicular to the stock axis. The introduction of added stresses and strains through the rotational motion of the die causes an increase in temperature, primarily in the stock core and in the zones of contact with the die bottom.

Figure 6 shows the fields of temperature distribution in the cross-section and on the surface of the forging for an analogous punch position, in the mobile and immobile die variants.

The temperature values that were recorded during simulation of forging in the immobile tool and during simulation of forging using the rotary die indicate significant differences along the entire length of the forging section.

In the zone of contact with the upper punch in the forging variant in Fig. 6a, temperature values oscillate in the range of 400-410°C, while for the forging variant in Fig. 6b, around 490°C. The distribution of temperature fields is layered for both cases. For the rotary die forging variant (Fig. 6b), individual layers formed by temperature fields are horizontal in character, and the value of temperature in the forging cross-section ranges from 475°C to 500°C.

Figure 7 shows the diagrams of the dependence of forging force on the punch path for the cases of forging a spiral gear wheel in an immobile die and in a rotary die for  $\omega = 0, 5, 10, 20$  rpm.

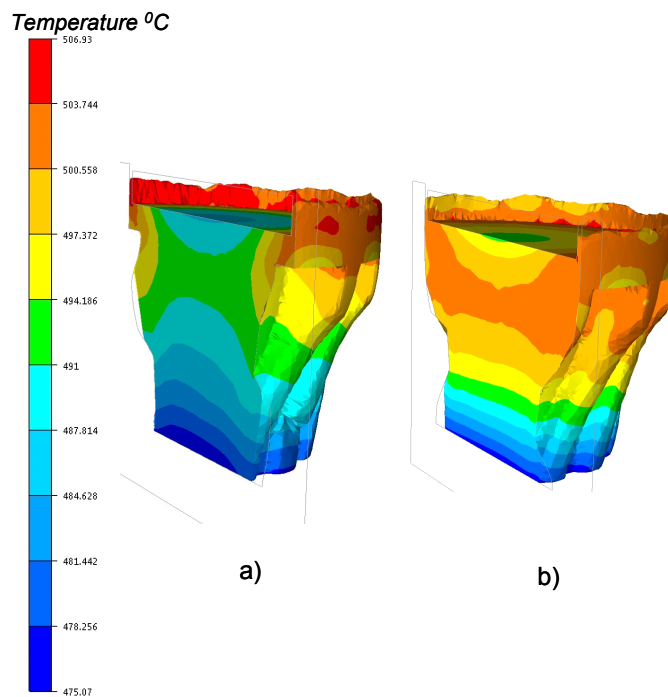


Fig. 6. Distribution of temperature with an analogous punch position for the spiral gear toothing variant: a) immobile die, b) rotary die at  $\omega = 10$  rpm

The numerical computations of the forging force as dependent on the punch path showed that setting the die in rotary motion resulted in a reduction of forging press pressure force

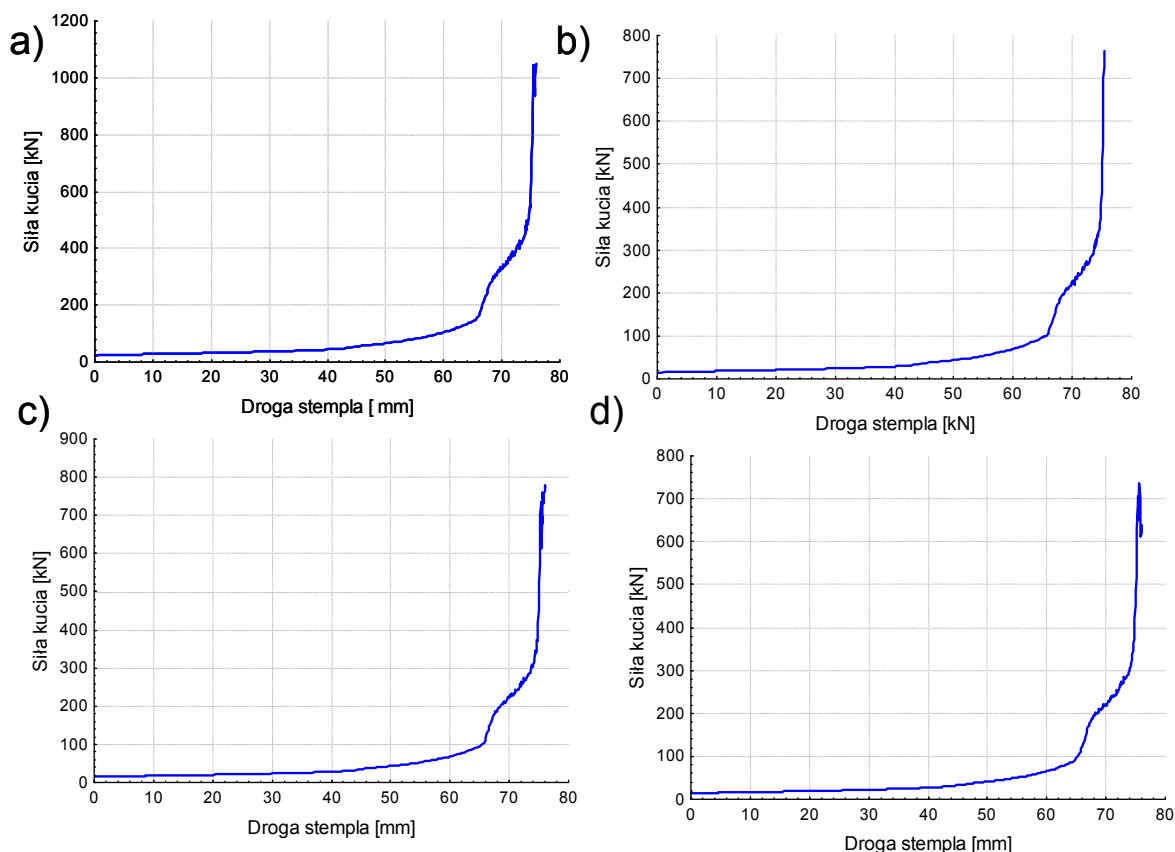


Fig. 7. Diagrams of the relationship of forging force versus punch path for a)  $\omega = 0$  rpm, b)  $\omega = 5$  rpm, c)  $\omega = 10$  rpm, d)  $\omega = 20$  rpm



by as much as approx. 35%. During forging a spiral gear using an immobile die, the forging force amounted to 1100 kN. For the rotary die forging variant for  $\omega = 20$  rpm, the forging force was 700 kN. A similar drop in forging force was noted for the straight and skew gear cases.

*The conical slidable and inverted die forging process.*

Figure 8a illustrates the process of forging according to the authors' method [6,21] in the slidable die (Fig. 3). According to this method, upsetting the bar on the gear base side resulted in

the deformation of the metal on both bar ends simultaneously. This caused one material layer to join to the other, which might, as a consequence, lead to the formation of internal defects in the form of lapping. To eliminate this phenomenon, the die was turned to face the punch with its conical part. As it flowed, the metal filled the die to form first the gear base and then, flowing partly radially and partly in the opposite direction to the tool motion, filled the die chamber to form gear teeth (Fig. 8b).

Figure 9 represents the distribution of temperature in the bar being deformed.

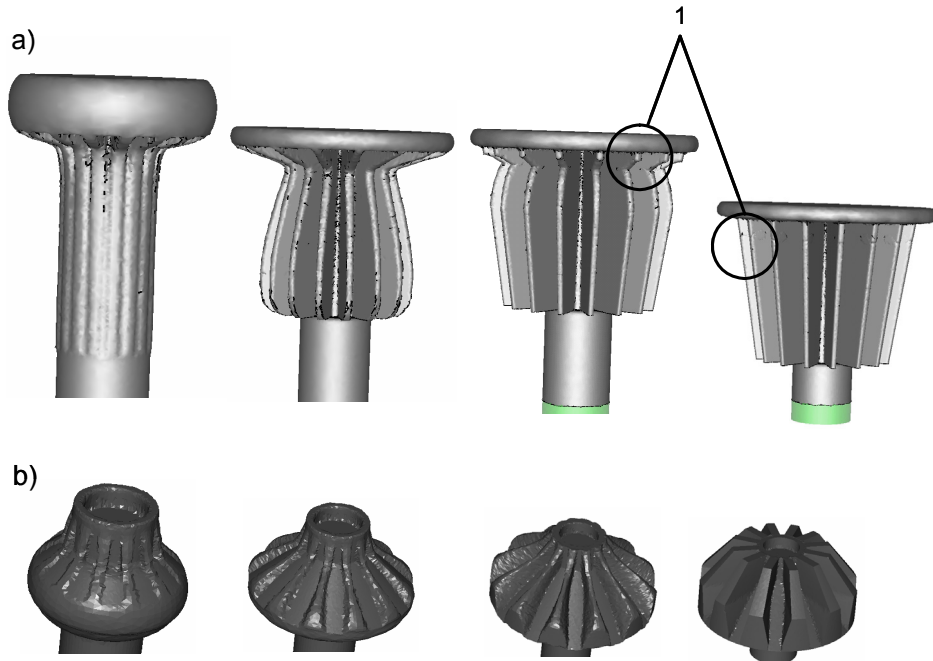


Fig. 8. Modelling of the process of gear forging: a) in the slidable die. 1 – formation of lapping defects; b) modelling of the process of gear forging in the inverted die

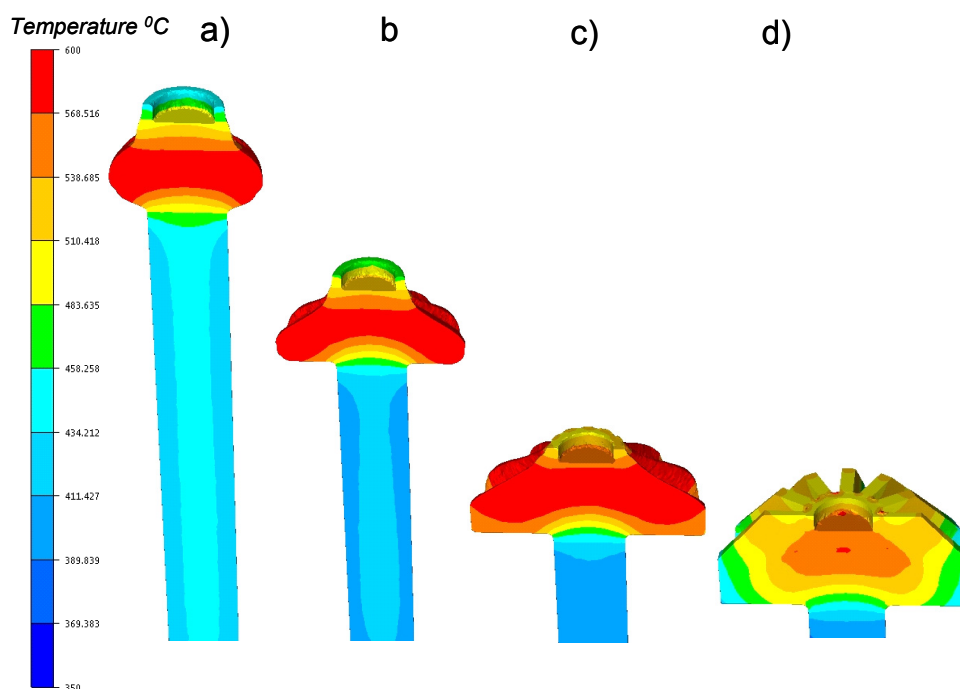


Fig. 9. Distribution of temperature in the cross-section of the bevel gear being formed

The employed forging speed of  $V = 20$  mm/s, from the point of view of forging industry applications, is relatively low. However, in spite of low tool speeds, the distribution of temperature in the forging throughout the process was required. The intensity of material flow in the upsetting region (Fig. 9a) and in the tooth formation through the radial and countercurrent flows (Fig. 9b,c) caused a temperature increment by approx.  $50^\circ\text{C}$  relative to the initial temperature. The largest metal overcooling layers occurred in the bar within the sleeve. The surface layer attained a temperature of approx.  $400^\circ\text{C}$ . Setting the die and the sleeve in motion caused a gradual deformation of the bar in the region of entry to the die. This resulted in a temperature increase in the lower die part from approx.  $400^\circ\text{C}$  to  $500\text{--}550^\circ\text{C}$ .

In computer simulations, the values of energy-force parameters were determined for the both processes of forging the gears shown in Fig. 8ab.

Figure 10 shows the diagram of the relationship of forging force versus punch path for the slidable die gear forging process.

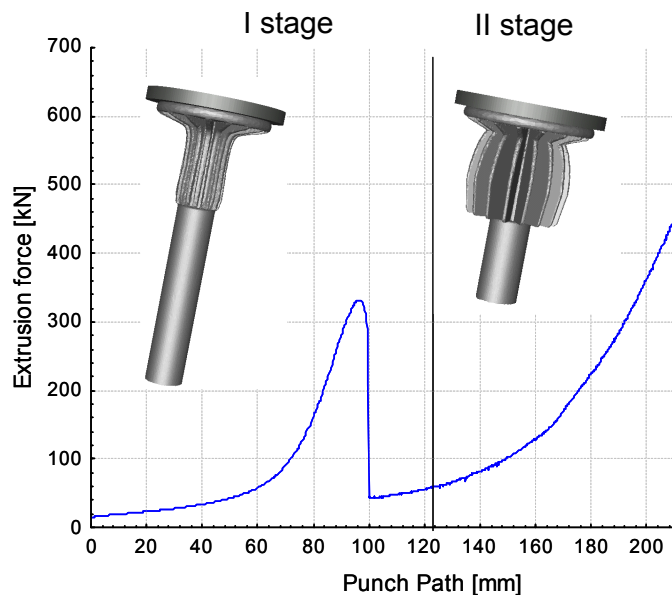


Fig. 10. Forging force as a function of punch path

The maximum extrusion force value at the first process step amounted to 332 kN. This value was attained when the punch approached the die at a distance equal to the gear base thickness. The gear ribs were finish formed at an extrusion force of 600 kN, that is after the punch had travelled a distance of 210 mm.

Figure 11 shows forging force as a function of punch path for the inverted die gear forging process.

The graph of the dependence of forging force on punch path (Fig. 11) is characteristic of this type of deformation patterns. Studies [1,7,8] report that, when using a tool with movable inserts for forging bottomed deep hollows, a relatively small force increase occurred initially, after which, upon starting up the tools, a decrease down to values even close to zero was noted; then, the force gradually increased up to a point at which finished product was obtained by holding down. In the gear forging process, the force attained a value of approx. 20 kN during bar

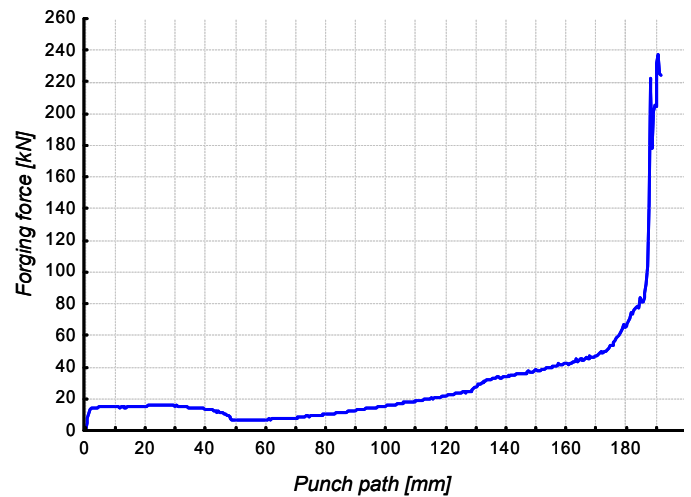


Fig. 11. Diagram of the relationship of forging force versus punch path

upsetting, and then, during radial and countercurrent metal flow in the impression, it reached a value of 80 kN. During holding down, the maximum forging pressure magnitude reached a level of 240 kN. With the size of a forging having a base radius of 65 mm and a height of 40 mm, these are relatively small forging force magnitudes. Presumably, the main causes of the low energy-force parameters are a unique strain pattern applied, high forging temperature and a small stock diameter of  $\phi 20$  mm, which is undoubtedly a great advantage of this process.

## 5. Summary

The advantage of the inverted die forging process over the slidable die forging process is obvious. The primary fundamental drawback of the process according to the scheme in Fig. 3 is the formation of defects, as revealed in Fig. 8a, which are due to the abnormal flow of metal in the gear rib formation region. The formation of defects in the form of lapping and forging discontinuities is almost certain in this case. Another advantage is the forging force which, for the process of gear production in the inverted die, is lower by about 200 kN. The reason is the scheme of gear rib formation. In the slidable die process, the formation of gear ribs proceeds through radial extrusion. By contrast, in the inverted die process, the ribs are obtained in the tool according to the scheme of indirect extrusion from a pre-upset bar.

In the rotary die gear production process, the maximum forging force was 330 kN. This is a value intermediate between the two examined gear forging methods. However, the deformation pattern itself is important here. Setting the die in rotary motion during the process of forging a prismatic bar caused it to rotate around its own axis. Thanks to this, torsion was introduced to the upsetting and radial extrusion deformation pattern. A considerable temperature increase within the forging and a forging force drop, compared to the immobile tool forging variant, were induced. It is worth noting that introducing a torsion pattern and added tangential stresses and strains may cause a change in mechanical properties as a result of material

structure refinement. In that case, it is possible to considerably improve the mechanical properties of the gear, which are a key parameter in the operation of such machine parts. Obviously, such presumptions can only be verified by physically making a forging and performing a metallographic analysis.

To sum up, from the point of view of tool design and force parameters, it is the inverted die method that would be the most effective in gear forging technology. From the point of view of the properties of the obtained product, on the other hand, this would probably be the rotary die forging method.

#### REFERENCES

- [1] A. Turno, R. Romanowski, M. Olszewski, *Obróbka Plastyczna kół zębatach*, Warszawa 1973
- [2] J. Sińczak, *Kucie dokładne*, Kraków 2011.
- [3] M. Zahn, *J. Mater. Process Tech.* **127**, 401-408 (2002).
- [4] J. Sińczak, *Kucie dokładne*, Kraków 2011.
- [5] J. Michalczyk, Method of producing a throughway sleeve, Polish Patent PL 221425.
- [6] J. Michalczyk, M. Suliga, The Method of producing the heat sink conical, Application Patent P416772.
- [7] A. Dziubińska, A. Gontarz, The Method of forming the heat sink, Polish Patent PL 219445.
- [8] G. Winiarski, A. Gontarz, Sposób i urządzenie do wyciskania wewnętrznego kołnierzy, Polish Patent PL 222169.
- [9] Z. Pater, J. Tomczak, A. Gontarz, Sposób wytwarzania kołnierzy czołowych w kształcie rozety trójramiennej, Polish Patent PL 220525.
- [10] G. Winiarski, A. Gontarz, A. Dziubińska, *Arch. Civ. Mech. Eng.* **17**, 4, (2012).
- [11] G. Winiarski, A. Gontarz. Sposób i urządzenie do wywijania kołnierza rolkami prowadzącymi, Polish Patent PL 219935.
- [12] J. Bartnicki, *Arch. Metall. Mater.* **57**, 4 (2012).
- [13] V.V. Dewiatov, H.S. Dyja, V.Y. Stolbow, *Modeling mathematical and optimization processes extrusions*, Częstochowa 2004.
- [14] A Gontarz, G. Winiarski, *Arch. Metall. Mater.* **60**, 3 (2016).
- [15] V.V. Dewjatow, J. Michalczyk, J. Rajczyk, *Teoretyczne podstawy i technologia procesów wyciskania*, Częstochowa 2011.
- [16] W. Libura, *Płynięcie metalu w procesie wyciskania*, Kraków 2011.
- [17] J. Sińczak, *Kucie dokładne*, Kraków 2011.
- [18] M. Pietrzyk, *The numerical methods in plastic working metals*, Kraków 1992.
- [19] H. Dyja, P. Szota, S. Mróz, *J. Mater. Process Tech.* **153**, 115-121 (2004).
- [20] J. Piwnik, *The Modeling processes plastic flow*, Białystok 1992.
- [21] J. Michalczyk, S. Mróz, P. Szota, The inverted conical die gear wheel forging method Application, Patent P427093.